A novel monoclinic phase and electrically tunable magnetism of van der Waals layered magnet $CrTe_2$

Qidi Ren(任启迪), Kang Lai(赖康), Jiahao Chen(陈家浩),
Xiaoxiang Yu(余晓翔)[†], and Jiayu Dai(戴佳钰)[‡]

Department of Physics, National University of Defense Technology, Changsha 410073, *China*

(Received 24 August 2022; revised manuscript received 8 October 2022; accepted manuscript online 19 October 2022)

Exploring the novel structural phase of van der Waals (vdW) magnets would promote the development of spintronics. Here, through first-principles calculations, we report a novel monoclinic structure of vdW layered 1T-$CrTe_2$, which is one of the popular vdW magnets normally exhibiting a trigonal structure. The new monoclinic phase emerges from a switchable magnetic state between ferromagnetism and antiferromagnetism through changing hole doping concentration, which suggests a practical approach to obtain such a structure. The results of phonon dispersion and energy analysis convince us that the monoclinic structure is a metastable phase even without hole doping. When the hole doping concentration increases, the stability analysis indicates the preference for a novel monoclinic phase rather than a conventional trigonal phase, and meanwhile, the magnetic properties are accordingly tuned. This work provides new insights into the phase engineering of the chalcogenide family and the electrical control of magnetism of vdW layered magnets.

Keywords: van der Waals magnets, magnetic transition, hole doping

PACS: 72.80.Ga, 75.30.Kz **DOI:** 10.1088/1674-1056/ac9b37

1. Introduction

The van der Waals (vdW) layered magnetic materials are gaining wide attention due to their low-dimensional electrical and magnetic properties and flexible fabrication, especially beneficial for the development of next-generation spintronic devices.[1,2] Enormous efforts have been devoted to the fabrication of the various systems and many magnetic materials have been reported, such as CrI_3,[3] Fe_3GeTe_2,[4,5] Cr_3Te_4,[6] $CrBr_3$,[7] and $Cr_2Ge_2Te_6$.[8] One of the merits that exploring the vdW layered magnetic system is that the magnetism can normally be tuned by customizing the stacking and doping of the system[9–11] or exerting optical method[12–15] as well as strain engineering,[16–18] which are extremely important for the efficient switching in building the magnetic memory devices. Although versatile methodologies have been explored,[19] the delicate tuning of the lattice structure to realize the dramatic change in the magnetism of the vdW layered system is still scarce.

Chromium-based chalcogenides attract great research interest due to their high-temperature magnetism.[20,21] Among them, bulk $CrTe_2$ is one of the popular vdW magnetic materials, which has a 1T-phase trigonal crystal structure (tr-$CrTe_2$) with a $P\bar{3}m1$ space group and possess ferromagnetic (FM) order.[22] Except for strain-induced antiferromagnetism in trigonal bulk $CrTe_2$,[23,24] to date, the new crystal structure of bulk $CrTe_2$ with antiferromagnetic (AFM) order has not been reported yet. Very recently, two crystal structures of trigonal and monoclinic Cr_5Te_8 have been selectively synthesized, however, both possess the same out-of-plane FM order.[25,26]

In this work, we predict a novel monoclinic crystal structure of vdW layered magnet 1T-$CrTe_2$ (m-$CrTe_2$), which possesses a $C2/m$ space group and antiferromagnetism. The lattice stability and magnetic order are confirmed based on calculated phonon dispersion and energy. We investigate the effects of hole doping on the lattice structure, phonon dispersion, energy, and magnetism. The results suggest that such structure and switching of magnetism could be realized by hole doping which is a practical approach reported in previous works.[9,27–29]

2. Computational methods

We performed first-principles calculations of bulk 1T-$CrTe_2$ using density functional theory (DFT)[30–32] in the generalized gradient approximation (GGA) for the exchange–correlation function implemented in the Vienna *ab initio* simulation package (VASP).[33,34] To consider the van der Waals interaction between layers, the projector augmented-wave method was employed with the Perdew–Burke–Ernzerhof (PBE)[35] optB88-vdW[36,37] for describing the exchange–correlation potential. The energy cutoff of the plane-wave basis was set at 650 eV. The atomic positions in the unit cell were fully relaxed until the force on each atom was smaller than 0.01 eV/Å. Therefore the obtained lattice parameters of tr-$CrTe_2$ are very close to the experimental values.[38] Phonon dispersions were calculated using the density functional perturbation theory (DFPT) method as implemented in

[†]Corresponding author. E-mail: xxyu@nudt.edu.cn
[‡]Corresponding author. E-mail: jydai@nudt.edu.cn

© 2023 Chinese Physical Society and IOP Publishing Ltd

the PHONOPY package.[39] The monkhorst-pack method was used to sample spatial integrals using the Gamma-centered grids of 12×12×8 for electronic structure calculations and 5×5×5 for phonon dispersion calculations. We used 2×2×1 supercells and fixed the spin directions of Cr atoms to realize the AFM state. In the calculations, hole doping was realized by reducing the total number of electrons. Meanwhile, charge correction was considered by compensating the background of the opposite charge to realize the charge neutral. The value of doping concentration denotes the reduced number of electrons in a primitive unit cell including one Cr atom and two Te atoms. The unit of doping concentration is $e^+/CrTe_2$. More details are shown in supplementary materials.

3. Results and discussion

We compare two crystal structures of tr-$CrTe_2$ and m-$CrTe_2$ as shown in Fig. 1. Both structures have a 1T-phase,[40] namely, one Cr atom is surrounded by six Te atoms octahedrally, as shown in Figs. 1(a) and 1(b). The space groups of the trigonal and monoclinic structure are $P\bar{3}m1$ and $C2/m$, respectively (see details in Table S1). The detailed lattice parameters are given in Table 1.

Table 1. Lattice parameters of tr-$CrTe_2$ and m-$CrTe_2$.

Phase	$a = b$ (Å)	c (Å)	$\alpha = \beta$ (°)	γ (°)
tr-$CrTe_2$	3.830	6.144	90.00	120.00
m-$CrTe_2$	3.728	6.331	90.96	118.02

The interlayer distance of m-$CrTe_2$ is larger than that of tr-$CrTe_2$, while the length of a ($a = b$) of m-$CrTe_2$ is smaller than that of tr-$CrTe_2$. The values of α ($\alpha = \beta$) and γ of m-$CrTe_2$ are 90.96° and 118.02°, respectively, which are different from 90° and 120° of tr-$CrTe_2$. Different from tr-$CrTe_2$, the adjacent layers show slight planar sliding in m-$CrTe_2$. Moreover, as denoted by pink solid lines in Figs. 1(c) and 1(d), the hexagon formed by three Te atoms and three Cr atoms and centered by a Te atom is regular in tr-$CrTe_2$ but irregular in m-$CrTe_2$. Due to the lattice distortion in m-$CrTe_2$, the fractional atomic coordinates of two Te atoms in the x and y directions deviate from 1/3 and 2/3 in tr-$CrTe_2$ (see details in Table S1). Therefore, it is proved that the new monoclinic phase is different from the conventional trigonal phase. Besides, recent experimental work[26] reported the synthesis of trigonal and monoclinic Cr_5Te_8 crystals. The difference between trigonal and monoclinic Cr_5Te_8 crystals is the distortion of Cr atoms. In this work, the differences between trigonal and monoclinic $CrTe_2$ crystals stem from the intralayer lattice distortion and interlayer sliding. Due to the changes in lattice parameters are too small, the differences in atomic structure in Fig. 1 are not obvious. As will be discussed later, figure S1 shows the obvious differences between two crystal structures with hole doping of 0.5 $e^+/CrTe_2$. To confirm the lattice stability, we calculate the phonon dispersion. As given in Figs. 1(e) and 1(f), all phonon modes are stable for tr-$CrTe_2$ and m-$CrTe_2$. Besides, the magnetic state of m-$CrTe_2$ is the AFM state, which will be discussed later.

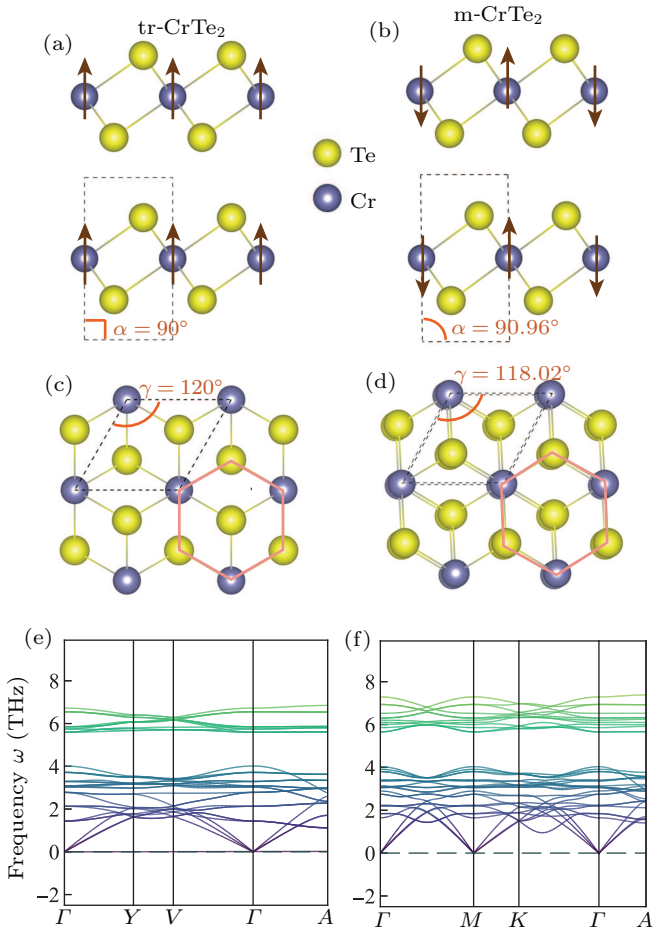


Fig. 1. Two crystal structures of bulk 1T-$CrTe_2$ along different axes, [(a), (c)] trigonal ($P\bar{3}m1$ phase group) and [(b), (d)] monoclinic ($C2/m$ phase group) structure. The black dashed lines denote the primitive cell. The pink solid lines highlight the hexagons formed by three Te atoms and three Cr atoms and centered by a Te atom. The brown arrows denote the spin directions of the Cr atoms. Phonon dispersion of (e) tr-$CrTe_2$ and (f) m-$CrTe_2$. All phonon modes are stable for both structures.

To find a possible approach for phase engineering, we focus on the electrical method which is a feasible tool to modulate the structural phase and magnetic properties.[27,28,41,42] We investigate the effect of hole doping on binding energy, phonon dispersion, and crystal structure. The energy difference between tr-$CrTe_2$ and m-$CrTe_2$, which is expressed by $\Delta E = E_m - E_{tr}$, is shown in Fig. 2 and Table S2. The energy difference decreases from positive to negative as the doping concentration increases. In the case without doping, tr-$CrTe_2$ is more stable than m-$CrTe_2$, indicating that the new m-$CrTe_2$ is a metastable structure. When the hole doping concentration is larger than 0.25 $e^+/CrTe_2$, $\Delta E < 0$, suggesting that m-$CrTe_2$ becomes more stable than tr-$CrTe_2$. The concentration of 0.25 $e^+/CrTe_2$ corresponds to a carrier density of 2.24×10^{14} e^+/cm^2 (9.36×10^{20} e^+/cm^3). Previous experimen-

tal works demonstrated that the carrier density could readily exceed the order of 10^{14} e^+/cm^2 by the electrostatic gating approach.[28,43–45] We also calculate and compare the energies of different magnetic configurations (shown in Fig. S2) and the energies of different magnetic orders for both tr-$CrTe_2$ and m-$CrTe_2$ structures (shown in Fig. S3). The calculation results support the above conclusion.

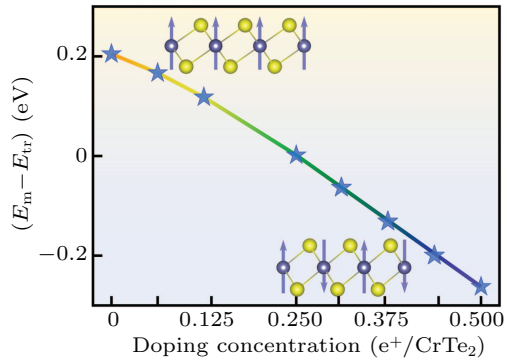


Fig. 2. The energy difference between tr-$CrTe_2$ and m-$CrTe_2$. The ground state energy of m-$CrTe_2$ is gradually lower than that of tr-$CrTe_2$ with hole-doping concentration increasing. The arrows denote the spin directions of the Cr atoms. The magnetic states of tr-$CrTe_2$ (in the upper left corner) and m-$CrTe_2$ (in the lower right corner) are FM and AFM, respectively.

Crystal structures also change with hole doping. Tables S3 and S4 give the lattice parameters of tr-$CrTe_2$ and m-$CrTe_2$ with different doping concentrations. The lattice structures of tr-$CrTe_2$ and m-$CrTe_2$ keep their space group symmetry unchanged, respectively. But the lattice lengths of both shrink gradually with the increase of doping concentration. When doping concentration reaches 0.5 $e^+/CrTe_2$, the reduction ratios of a, b, and c for tr-$CrTe_2$ (m-$CrTe_2$) are 9.1% (9.5%), 9.1% (9.5%), and 7.8% (8.6%), respectively. As the doping concentration increase from 0 to 0.5 $e^+/CrTe_2$, the values of α ($\alpha = \beta$) and γ of m-$CrTe_2$ increase from 90.96° to 91.77° and from 118.02° to 116.46°, respectively, and the volume decreases by 24.5%. Previous works also reported comparable electrical-doping-induced volume change in other layered materials.[46] The extent of lattice distortion in m-$CrTe_2$ becomes larger with the increasing hole doping concentration. We depicted the two crystal structures with hole doping of 0.5 $e^+/CrTe_2$. As one can see in Fig. S1, the differences between the two crystal structures become obvious. Here, we should leave the suspense of why the magnetism of m-$CrTe_2$ is AFM, which will be discussed further later.

Except for the energy stability, one also needs to confirm the lattice stability via phonon dispersion.[47] Figure 3 compares the phonon dispersion of tr-$CrTe_2$ and m-$CrTe_2$ with different doping concentrations. As the doping concentration increases, all phonon modes of m-$CrTe_2$ remain stable and show hardening. For tr-$CrTe_2$, most phonon modes show hardening. However, when doping concentration reaches 0.25 $e^+/CrTe_2$, two phonon modes Γ_1 and A_1 become unstable. As doping concentration increases to 0.5 $e^+/CrTe_2$, there are three unstable phonon modes: Γ_1, M_1, and A_1. These unstable phonon modes are stabilized by interlayer sliding and intralayer displacive distortion.[48,49] Therefore, the results imply that hole doping could be a possible approach to accessing the novel m-$CrTe_2$ structure.

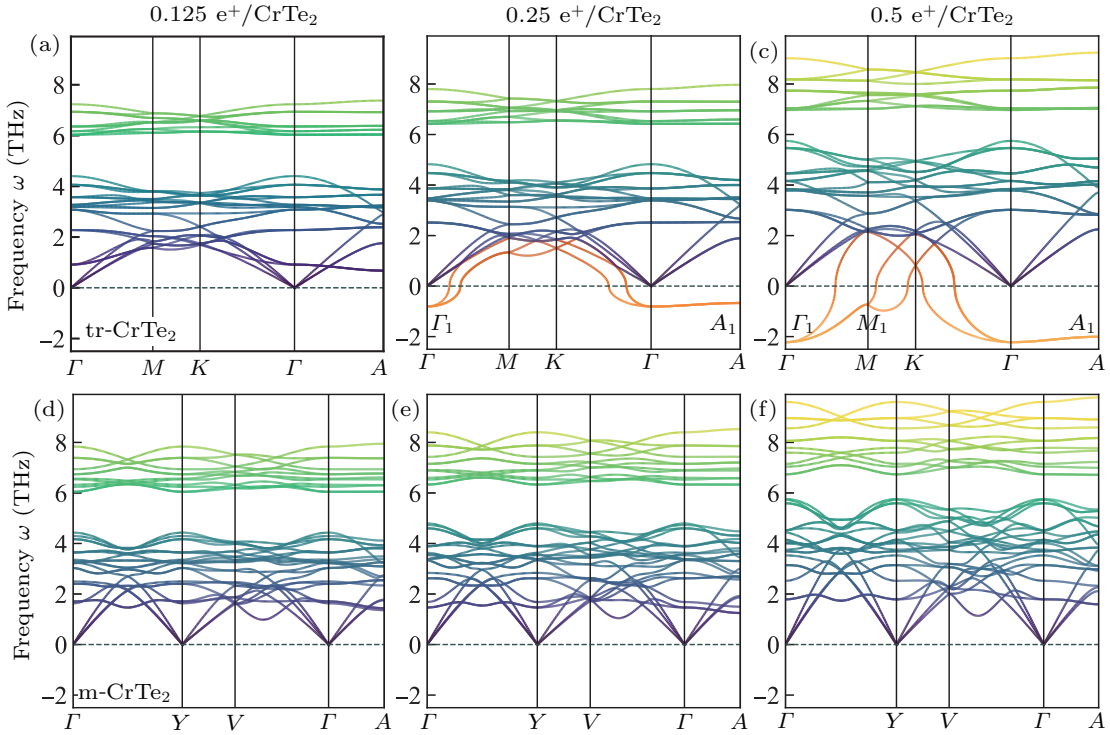


Fig. 3. Phonon dispersion of (a)–(c) tr-$CrTe_2$ and (d)–(f) m-$CrTe_2$ with different doping concentrations. For tr-$CrTe_2$, unstable phonon modes appear when doping concentration increases, and most phonon modes show hardening. All phonon modes of m-$CrTe_2$ remain stable and show hardening as the doping concentration increases.

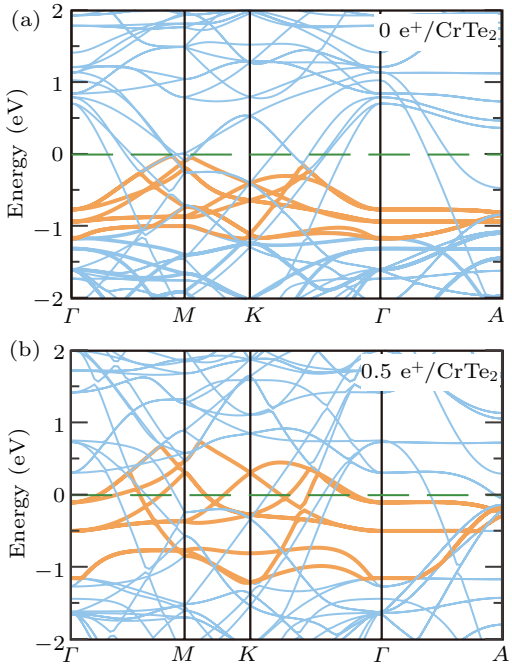


Fig. 4. Electronic bands of (a) undoped tr-$CrTe_2$ and (b) tr-$CrTe_2$ in hole doping of 0.5 $e^+/CrTe_2$. After hole doping, there is more electron occupation near the Fermi level, resulting in strong electron–phonon interactions and phonon softening in Fig. 3.

To shed light on the mechanism of phonon softening in hole-doped tr-$CrTe_2$, we calculate the electronic band structures of tr-$CrTe_2$ with different doping concentrations, as shown in Figs. 4 and S4. The anomalous phonon softening is attributed to the hole-doping-induced phonon Kohn anomaly. As the doping concentration increases, the spin-up and spin-down electron states of the Cr atoms shift towards the Fermi level. The energy shifts of electron states of the Te atoms are relatively small. For tr-$CrTe_2$ in hole doping of 0.5 $e^+/CrTe_2$, there are more electronic bands near Fermi level compared with undoped one. The high symmetry points of unstable phonon modes (Γ_1, M_1, and A_1) are consistent with the reciprocal-space positions where the electronic bands near the Fermi level locate. The increase of electron occupation near the Fermi level leads to enhanced electron screening and electron-phonon coupling, thus weakening the interatomic interactions and softening phonon modes at corresponding specific high-symmetry points.[50]

Apart from structural change, the magnetic preference induced by hole doping is also identical to many other vdW magnets. First, we focus on the magnetic moment of different types of atoms, as shown in Figs. 5 and S5, to give a global scope on the magnetic state of the system while exerting hole-doping. The magnetic moment of the system is mainly contributed by d electrons of Cr atoms (Cr-d electrons), which can be explained by Stoner instability.[51] As the doping concentration increases, the magnetic moment decreases gradually except for the p electrons of Te atoms (Te-p electrons) in AFM states. The magnetic moments of Cr and Te atoms are in opposite directions.

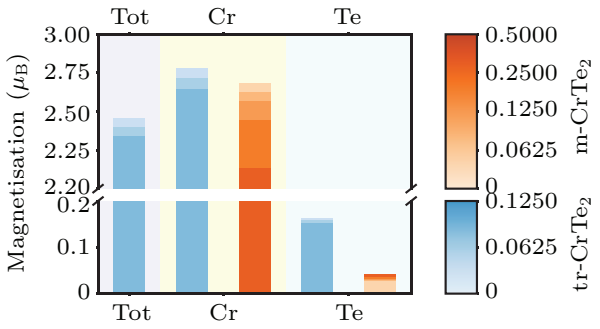


Fig. 5. Magnetic moment of tr-$CrTe_2$ and m-$CrTe_2$ with different doping concentrations. The magnetic moment decreases as doping concentration increases. The main contribution to the total magnetic moment is from Cr atoms.

Then we compare the magnetic states in the matrix of tr-$CrTe_2$, giving the electron density of states (DOS) of spin polarization state as hole-doping increases. For tr-$CrTe_2$, in Figs. 6 and S6, the DOS of Cr-d electrons with opposite spin is asymmetric. The spin polarization of Cr-d electrons can be regarded as the main contribution to the magnetism of $CrTe_2$. As the hole-doping concentration increases, the ferromagnetism decreases gradually, evidenced by the DOS smoothing and the peak moving towards the Fermi level, suggesting a reverse mechanism of the Stoner ferromagnetism.[41] On the other hand, when repeating the DOS calculations in the matrix of m-$CrTe_2$, the spin polarization reflected by DOS exhibits antiferromagnetic alignment, as shown in Fig. S7. From the point of view of the shift away from the Fermi level, the partial DOS reflects the delocalization of electrons, and the charge redistribution results in the decrease of the moment when pumping out the electrons from the system.

Here are some further discussions on the cause of the magnetic behavior when performing the calculation from the perspective of exchange competition.[24] In the normal tr-$CrTe_2$ without doping, two adjacent Cr atoms are bonded to each other and bridged by a Te atom, where the superexchange interaction mediated via the Te atom gives rise to ferromagnetism. As the doping suggests, the distance between two Cr atoms changes dramatically when the concentration of the doped holes is increased, as shown in Table S5. When the distance between two adjacent Cr atoms is short enough, the contribution of direct interaction between Cr atoms will not be negligible. Pauli repulsion tells us that antiferromagnetism should be the ground state. Therefore, the competition between the AFM exchange of the Cr–Cr and FM superexchange of Cr–Te–Cr should be considered during the hole-doping process. When the doping exceeds a threshold to reach the critical bonding distance, the AFM interaction will dominate. This mechanism has also been suggested by previous studies on $CrTe_2$, where strain and phase transition can similarly affect the ferromagnetism of $CrTe_2$.[23]

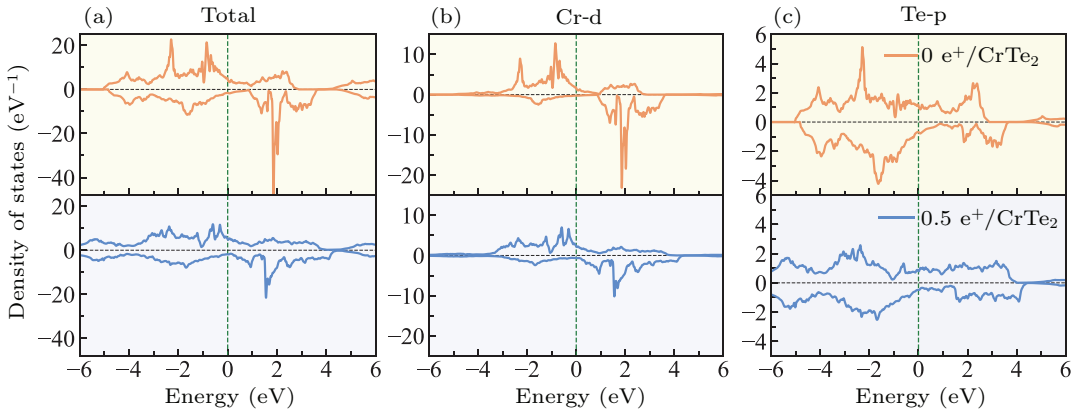


Fig. 6. Electron density of states (DOS) of tr-$CrTe_2$. The green dotted lines represent Fermi levels. (a) Total DOS and (b) DOS of Cr-d electrons show a similar distribution. The peaks move closer to the Fermi level with the doping concentration increasing. Results of two doping concentrations (0 and 0.5 $e^+/CrTe_2$) are shown to exemplify the doping effect on phonon dispersion and electronic structure (see more results in Figs. S6 and S7).

4. Conclusions

In conclusion, we predict a new monoclinic structure of vdW layered magnet $CrTe_2$. Distinct from the conventional trigonal structure with ferromagnetism, the new structure exhibits a $C2/m$ space group and antiferromagnetism, which emerges when exerting the hole doping. We verified the stability of the new phase through phonon dispersion and energy calculation. As hole-doping concentration increases, several phonon modes of tr-$CrTe_2$ become unstable, while those of m-$CrTe_2$ remain stable. We calculate the electronic structures to reveal the mechanism of this phase instability. We find that the hole-doping-induced phonon Kohn anomaly is responsible for the instability of certain phonon modes. Furthermore, the volume and other lattice parameters change with increasing hole-doping concentration. For the m-$CrTe_2$, the volume is reduced by 24.5% for doping concentration of 0.5 $e^+/CrTe_2$. Accompanied by the structural distortion, the competition between bonding interaction and direct interaction of Cr atoms contributes to the change of magnetism. Although the large lattice distortion leads to a large change in the magnetic property, we propose to exploit such effect as a possible technique to realize the phase engineering of vdW layered magnets, which could be employed as an effective method of magnetic state switching.

Acknowledgements

Project supported by the National Key Research and Development Program of China (Grant No. 2017YFA0403200), the National Natural Science Foundation of China (Grant No. 11774429), the NSAF (Grant No. U1830206), and the Science and Technology Innovation Program of Hunan Province, China (Grant No. 2021RC4026).

References

[1] Gibertini M, Koperski M, Morpurgo A F and Novoselov K S 2019 *Nat. Nanotechnol.* **14** 408
[2] Jiang X, Liu Q X, Xing J P, Liu N S, Guo Y, Liu Z F and Zhao J J 2021 *Appl. Phys. Rev.* **8** 031305
[3] Huang B, Clark G, Navarro-Moratalla E, Klein D R, Cheng R, Seyler K L, Zhong D, Schmidgall E, McGuire M A, Cobden D H, Yao W, Xiao D, Jarillo-Herrero P and Xu X 2017 *Nature* **546** 270
[4] Fei Z Y, Huang B, Malinowski P, Wang W, Song T C, Sanchez J, Yao W, Xiao D, Zhu X Y, May A F, Wu W, Cobden D H, Chu J H and Xu X D 2018 *Nat. Mater.* **17** 778
[5] Chen X, Lin Z Z and Cheng L R 2021 *Chin. Phys. B* **30** 047502
[6] Li B, Deng X, Shu W, *et al.* 2022 *Mater. Today* **57** 66
[7] Wang H D, Lei P H, Mao X Y, Kong X, Ye X Y, Wang P F, Wang Y, Qin X, Meijer J, Zeng H L, Shi F Z and Du J F 2022 *Chin. Phys. Lett.* **39** 047601
[8] Gong C, Li L, Li Z L, Ji H W, Stern A, Xia Y, Cao T, Bao W, Wang C Z, Wang Y, Qiu Z Q, Cava R J, Louie S G, Xia J and Zhang X 2017 *Nature* **546** 265
[9] Jiang S W, Li L Z, Wang Z F, Mak K F and Shan J 2018 *Nat. Nanotechnol.* **13** 549
[10] Lai X B, Wang Y H, Shi X L, Li D Y, Liu B Y, Wang R M and Zhang L W 2016 *Chin. Phys. Lett.* **33** 067202
[11] Zhao G, Cheng X M, Jun T H, Du B Q and Liang X Y 2011 *Chin. Phys. Lett.* **28** 127203
[12] Liu B, Liu S S, Yang L, Chen Z D, Zhang E, Li Z, Wu J, Ruan X Z, Xiu F X, Liu W Q, He L, Zhang R and Xu Y B 2020 *Phys. Rev. Lett.* **125** 267205
[13] Kobayashi S, Katayama N, Manjo T, Ueda H, Michioka C, Sugiyama J, Sassa Y, Forslund O K, Månsson M, Yoshimura K and Sawa H 2019 *Inorg. Chem.* **58** 14304
[14] Sun X N, Qu Z M, Wang Q G, Yuan Y and Liu S H 2019 *Acta Phys. Sin.* **68** 107201 (in Chinese)
[15] Yu Y, Zhang W J, Zhao W Y, Lin X, Jin Z M, Liu W M and Ma G H 2019 *Acta Phys. Sin.* **68** 017201 (in Chinese)
[16] Vishkayi S I, Torbatian Z, Qaiumzadeh A and Asgari R 2020 *Phys. Rev. Mater.* **4** 094004
[17] Cheng K Q, Zhou B J, Wang C X, Zou S, Pan Y P, He X B, Zhang J, Lu F J, Wang L, Shi Y G and Luo Y K 2022 *Chin. Phys. B* **31** 67104
[18] Zhang L, He D W, He J Q, Fu Y and Wang Y S 2019 *Chin. Phys. B* **28** 087201
[19] Xie W Q, Lu Z W, He C C, Yang X B and Zhao Y J 2021 *J. Phys.: Condens. Matter* **33** 215803
[20] Zhou J, Song X H, Chai J W, Wong N L M, Xu X G, Jiang Y, Feng Y P, Yang M and Wang S J 2022 *J. Alloys Compd.* **893** 162223
[21] Pan L F, Wen H Y, Huang L, Chen L, Deng H X, Xia J B and Wei Z M 2019 *Chin. Phys. B* **28** 107504
[22] Sun X D, Li W Y, Wang X, *et al.* 2020 *Nano Res.* **13** 3358
[23] Lv H Y, Lu W J, Shao D F, Liu Y and Sun Y P 2015 *Phys. Rev. B* **92** 214419
[24] Li Q Q, Li S, Wu D, Ding Z K, Cao X H, Huang L, Pan H, Li B, Chen K Q and Duan X D 2021 *Appl. Phys. Lett.* **119** 162402
[25] Lukoschus K, Kraschinski S, Näther C, Bensch W and Kremer R K 2004 *J. Solid State Chem.* **177** 951
[26] Tang B, Wang X, Han M, Xu X, Zhang Z, Zhu C, Cao X, Yang Y, Fu Q, Yang J, Li X, Gao W, Zhou J, Lin J and Liu Z 2022 *Nat. Electron.* **5** 224

[27] Wang Y, Xiao J, Zhu H Y, Li Y, Alsaid Y, Fong K Y, Zhou Y, Wang S Q, Shi W, Wang Y, Zettl A, Reed E J and Zhang X 2017 *Nature* **550** 487

[28] Verzhbitskiy I A, Kurebayashi H, Cheng H X, Zhou J, Khan S, Feng Y P and Eda G 2020 *Nat. Electron.* **3** 460

[29] Feng H L, Li Y, Shi Y G, Xie H Y, Li Y Q and Xu Y 2022 *Chin. Phys. Lett.* **39** 077501

[30] Hohenberg P and Kohn W 1964 *Phys. Rev. B* **136** B864

[31] Dai J Y, Yuan J M and Giannozzi P 2009 *Appl. Phys. Lett.* **95** 232105

[32] Lin C J, Zheng F and Zhu Z Z 2019 *Acta Phys. Sin.* **68** 157201 (in Chinese)

[33] Kresse G and Hafner J 1993 *Phys. Rev. B* **47** 558

[34] Kresse G and Furthmüller J 1996 *Phys. Rev. B* **54** 11169

[35] Perdew J P, Ernzerhof M and Burke K 1996 *J. Chem. Phys.* **105** 9982

[36] Klimeš J, Bowler D R and Michaelides A 2009 *J. Phys.: Condens. Matter* **22** 022201

[37] Zeng F, Zhang W B and Tang B Y 2015 *Chin. Phys. B* **24** 097103

[38] Freitas D C, Weht R, Sulpice A, Remenyi G, Strobel P, Gay F, Marcus J and Nunez-Regueiro M 2015 *J. Phys.: Condens. Matter* **27** 176002

[39] Togo A and Tanaka I 2015 *Scr. Mater.* **108** 1

[40] Cao Y F, Cai K M, Li L J, Lu W J, Sun Y P and Wang K Y 2014 *Chin. Phys. Lett.* **31** 077203

[41] Cao T, Li Z L and Louie S G 2015 *Phys. Rev. Lett.* **114** 236602

[42] Fan G Z, Chen R Y, Wang N L and Luo J L 2015 *Chin. Phys. Lett.* **32** 077203

[43] Ye J T, Craciun M F, Koshino M, Russo S, Inoue S, Yuan H T, Shimotani H, Morpurgo A F and Iwasa Y 2011 *Proc. Natl. Acad. Sci. USA* **108** 13002

[44] Efetov D K and Kim P 2010 *Phys. Rev. Lett.* **105** 256805

[45] Li Y, Duerloo K A N, Wauson K and Reed E J 2016 *Nat. Commun.* **7** 10671

[46] Wu B Z, Cai X X, Shui L Q, Gao E and Liu Z 2021 *J. Phys. Chem. C* **125** 1060

[47] Zhang Q, Yu X X, Zeng Q Y, Zhang H Y, Zhang S, Gao C, Kang D D, Wu J H and Dai J Y 2022 *Front. Phys.* **10** 838568

[48] Aseginolaza U, Bianco R, Monacelli L, Paulatto L, Calandra M, Mauri F, Bergara A and Errea I 2019 *Phys. Rev. Lett.* **122** 075901

[49] Guan M X, Liu X B, Chen D Q, Li X Y, Qi Y P, Yang Q, You P W and Meng S 2022 *Phys. Rev. Lett.* **128** 015702

[50] Kohn W 1959 *Phys. Rev. Lett.* **2** 393

[51] Stollhoff G, Oleś A M and Heine V 1990 *Phys. Rev. B* **41** 7028